

STATISTICAL DISTRIBUTIONS OF OPTICAL FLARES FROM GAMMA-RAY BURSTS

SHUANG-XI YI^{1,3,4}, HAI YU^{2,4}, F. Y. WANG^{2,4}, AND ZI-GAO DAI^{2,4}¹College of Physics and Engineering, Qufu Normal University, Qufu 273165, China;²School of Astronomy and Space Science, Nanjing University, Nanjing 210093, China; fayinwang@nju.edu.cn³GXU-NAOC Center for Astrophysics and Space Sciences, Department of Physics, Guangxi University, Nanning 530004;⁴Key laboratory of Modern Astronomy and Astrophysics (Nanjing University), Nanjing 210093, China.

ABSTRACT

We statistically study gamma-ray burst (GRB) optical flares from the *Swift*/UVOT catalog. We compile 119 optical flares, including 77 flares with redshift measurements. Some tight correlations among the time scales of optical flares are found. For example, the rise time is correlated with the decay time, and the duration time is correlated with the peak time of optical flares. These two tight correlations indicate that longer rise times are associated with longer decay times of optical flares, and also suggest that broader optical flares peak at later times, which are consistent with the corresponding correlations of X-ray flares. We also study the frequency distributions of optical flare parameters, including the duration time, rise time, decay time, peak time and waiting time. Similar power-law distributions for optical and X-ray flares are found. Our statistic results imply that GRB optical flares and X-ray flares may share the similar physical origin and both of them are possibly related to central engine activities.

Subject headings: gamma rays: general — radiation mechanism: non-thermal

1. INTRODUCTION

Gamma-ray bursts (GRBs) are the most luminous phenomena occurring at cosmological distances. It is well known that the prompt gamma-ray emission is produced by internal dissipation processes within the relativistic ejecta (Piran 2004; Mészáros 2006; Zhang 2007; Kumar & Zhang 2015), while the broadband afterglows are usually interpreted as the interaction of an ultra-relativistic ejecta with the ambient medium (Mészáros & Rees 1997; Sari 1998). The successful launch of the *Swift* satellite in 2004 (Gehrels et al. 2004) has greatly improved our understanding of GRB physics. Since its rapid response, *Swift* could quickly allow the X-Ray Telescope (XRT) and the Ultraviolet/Optical Telescope (UVOT) to localize a GRB position and begin to observe the afterglow (Burrows et al. 2005a; Roming et al. 2005).

Some new phenomena are also discovered in the *Swift* satellite era, while the most intriguing phenomenon is the erratic flares of the “canonical” X-ray light curve, observed in the early X-ray afterglow phase (Burrows et al. 2005b; Zhang et al. 2006; Nousek et al. 2006). Those erratic X-ray flares usually happen at $\sim 10^2 - 10^5$ s after the prompt emission (Falcone et al. 2007; Chincarini et al. 2007, 2010; Swenson & Roming 2014), and are observed in both long and short GRBs (Romano et al. 2006; Falcone et al. 2006; Campana et al. 2006; Margutti et al. 2011). Since flares appear to come from a distinct emission mechanism than the underlying afterglow emission, and are seen in both long and short GRBs, it is generally supposed to be powered by the central engine activities. Therefore, X-ray flares and the prompt gamma-ray emission may have the similar physical origins (Burrows et al. 2005b; Fan & Wei 2005a; Falcone et al. 2006, 2007; Zhang et al. 2006; Nousek et al. 2006; Wu et al. 2006; Chincarini et al. 2007, 2010; Abdo et al. 2011; Troja et al. 2015; Yi et al. 2015; Mu et al. 2016a). Interestingly, flares also appear in the UV/optical band. Li et

al. (2012) selected a group of optical light curves with flares, and suggested that optical flares are also related to the erratic behavior of the central engine, which are similar to X-ray flares. Flares are both observed in the X-ray as well as the UV/optical bands, but the number of GRBs with optical flares is much smaller than that of GRBs with X-ray flares.

Flares are common astrophysical phenomena throughout the universe. Some studies on X-ray flares from astrophysical systems have been carried out (Wang et al. 2015). Wang & Dai (2013) selected 83 GRB X-ray flares and 11595 solar X-ray flares, and performed a statistical comparison between them. They found the energy, duration, and waiting-time distributions of GRB X-ray flares are similar to those of solar flares, which suggest a similar physical origin of the two kinds of flares. Some works using different methods and data also obtain a similar result (Aschwanden 2011; Wang et al. 2015; Harko et al. 2015; Guidorzi et al. 2015). These results are supported by Yi et al. (2016), who studied all significant X-ray flares from GRBs observed by *Swift* until March 2015, and obtained 468 bright X-ray flares, including 200 flares with redshifts. They found that there are four power-law distributions with different indices between X-ray flares and solar flares, including power-law distributions of energies, durations, peak fluxes and waiting times. Besides, they also studied the peak times, rising times and decay times of GRB X-ray flares, and found all of them show the power-law distributions. These similar statistical distributions between solar flares and GRB X-ray flares suggest both of them could be produced by magnetic reconnection, and also could be explained by a fractal diffusive, self-organized criticality model (Aschwanden 2011; Wang & Dai 2013; Harko et al. 2015; Dănilă et al. 2015; Yi et al. 2016). Interestingly, some theoretical models have been proposed that GRB X-ray flares could be powered by magnetic reconnection events (Giannios 2006; Dai et

al. 2006; Zhang & Yan 2011; Mu et al. 2016b).

In this paper, we investigate the optical flares observed by *Swift*/*UVOT* and study the distributions of optical flare parameters, such as duration times, rise times, decay times, peak times and waiting times. Since optical flares and X-ray flares may have a common physical origin, both of them may have similar distributions of the parameters. This paper is organized as follows. In Section 2, we present the selected GRB sample. In section 3, we study some correlations between parameters of optical flares. The distributions of flare parameters are discussed in Section 4. Discussion is given in Section 5. Section 6 presents conclusions. A concordance cosmology with parameters $H_0 = 71 \text{ km s}^{-1} \text{ Mpc}^{-1}$, $\Omega_M = 0.30$, and $\Omega_\Lambda = 0.70$ is adopted in all part of this work.

2. DATA

We extensively search for the optical flares of GRBs. Since the fraction of GRBs with optical flares is much smaller than that of X-ray flares, we mainly focus on GRBs detected by *Swift*/*UVOT*. Swenson et al. (2013) carefully studied the second UVOT GRB afterglow catalog, which provides a complete data set of fitted UVOT light curves for both long and short GRBs observed by *Swift* from 2005 April through 2010 December (Roming et al. 2009). They found more than one hundred unique potential flares in 68 different optical light curves, and obtained the starting time, peak time and end time of optical flares. We consider the full sample containing 119 optical flares (see their Table 2), including 77 flares with redshifts. These optical flares usually contain a complete structure, including remarkable rising and decaying phase. Figure 1 shows an sample of the optical flares. Most GRBs have a single optical flare, but some of them have several optical flares.

We carefully study the timescales of optical flares, such as waiting time, duration time, peak time, rise time and decay time. The time parameters of optical flares are derived as follows, which also can be seen in Yi et al. (2016). The rise time can be derived by $T_{rise} = T_{peak} - T_{start}$, the decay time $T_{decay} = T_{stop} - T_{peak}$ and the duration time $T_{Duration} = T_{stop} - T_{start}$, where T_{start} , T_{peak} and T_{stop} are the starting time, peak time and end time of flares, respectively. They are all listed in Table 2 of Swenson et al. (2013). The waiting time for one flare is defined as $T_{waiting} = T_{start,i+1} - T_{start,i}$, where $T_{start,i+1}$ is the observed start time of the $i + 1$ th flare, and $T_{start,i}$ is the observed start time of the i th flare. All the optical flare properties should be transferred into the source rest frame, if they have redshift measurements in the following analysis. For the first flare appearing in an optical afterglow, the rest-frame waiting time is simply taken as $T_{start}/(1+z)$, where z is redshift. We next study the frequency distributions of the duration time, waiting time, rise time, decay time and peak time of optical flares. Since optical flares and X-ray flares may have a common physical origin, we will compare the results of optical flares with X-ray flares, and check whether both of them show similar distributions of parameters.

3. PARAMETERS OF OPTICAL FLARES AND CORRELATIONS

Figure 2 shows the waiting time and peak time histogram distributions of the optical flares. The waiting

times of optical flares range from 10 s to 10^6 s after the GRB trigger, mainly from 10^2 s to 10^3 s, which is similar to the distribution of X-ray flares. The peak time T_{peak} of optical flare is in the range of 10^2 s to 10^6 s, mainly in 10^2 s to 10^3 s, occurring at the early time of the optical afterglow, which is consistent with the peak time distribution of X-ray flares. The optical smooth onset bumps are also peaking at the early time of the afterglow, but the optical flares and onset bumps are different from each other. According to the standard forward shock model, the onset of GRB afterglow is characterized by a smooth bump in the early afterglow when the ultra-relativistic fireball is decelerated by the circumburst medium, and these features are well consistent with the forward shock models (Molinari et al. 2007; Liang et al. 2010, 2013; Yi et al. 2013).

We use the simple linear regression analysis for parameter fitting¹ (Chatterjee et al. 2000), which is a linear regression model with a single variable. In this paper, we only consider correlations between two parameters of optical flares. So the simple linear regression method is adequate. Interestingly, these correlations have been found in X-ray flares of GRBs (Chincarini et al. 2007, 2010; Yi et al. 2016). Therefore, similar correlations could be expected in the optical flares. If treating multivariate correlations, multiple regression method should be used. Figure 3 presents the strong correlation between the rise and decay times of the optical flares. The rise time is tightly correlated with the decay time with the slope index of 0.99. There is also a strong correlation between the duration time and the peak time, with the slope index of 1.11. These two strong correlations indicate that longer rise times are associated with longer decay times for optical flares, and also suggest that broader optical flares peak at later times. The two correlations of optical flares are in good agreement with the corresponding correlations of X-ray flares, which can be seen from Figure 3 of Yi et al. (2016). The best fitting results of the four correlations are shown in Table 1. These tight correlations suggest that the structures of the optical and X-ray flares are similar, indicating a similar physical origin of them. Besides, Figure 3 also exhibits the correlations between the waiting time and other parameters of the optical flares. The waiting time is correlated with both the peak time and the duration time of optical flares, which indicates a longer waiting time tends to peak at a later time with a longer duration time, which are also consistent with the correlations of X-ray flares. In the fitting, the errors of parameters are not considered. Because there are no parameter errors reported in the optical flares from the second UVOT GRB Catalog (Swenson et al. 2013). In order to test whether the fitting results are biased by parameter errors, we assume the errors are randomly changed in the 10 – 20% range of the original value. We take the $T_{waiting} - T_{peak}$ correlation as an example. After considering the parameter errors, we find that the best-fitted power-law index is 0.90 using the method proposed by Kelly (2007). So this result is consistent with that in Table 1.

However, the start and end times of flares are affected by the observational temporal gaps in the Swift light curve, so the time scales of flares, such as, the rise time,

¹ https://en.wikipedia.org/wiki/Simple_linear_regression

decay time and duration time, may be also changed. In order to test this observational bias for the four correlations, we simulate 10^4 times for each correlation. In each simulation, the time scales will be randomly changed in the 0 – 10% range of the original value. Then we refit the correlations. The best-fitting results are shown in Figure 4. From this figure, we can see that the fitting results from simulations are slightly different from the value derived from observation data. They are consistent with each other at 1σ confidence level.

Some other instrumental and observational biases, which tend to disfavor flares with short durations at late times or smooth flares with long durations, will affect the observational correlations. Because the UVOT collects data in event mode during the first ~ 1000 s, while later observations are performed in image mode. The former mode has full temporal resolution, the latter mode integrates light over the whole exposure. For this reason, flares with a duration of 100-200 s cannot be easily detected at late times, because the observations average the emission over several hundreds of seconds. Furthermore, the identification of a flare requires also the identification of the underlying continuum. A smooth, longer-lasting flare could be more easily misclassified as continuum and therefore missed. Overall, the temporal correlations of optical flares may derive from instrumental and observational biases, especially for those flares with short durations but at late time, or smooth flares with long durations. We take the $T_{Duration} - T_{peak}$ correlation as an example. In order to test the two biases, we provide two groups of simulation data in Figure 5, i.e., optical flares with short durations at late times for the first bias (the red circles), and the smooth flares with long duration times for the second bias (the blue circles). For the first bias, we simulate 500 optical flares with $100s < T_{Duration} < 300s$ and $10^5s < T_{peak} < 10^6s$. For the second bias, we simulate 500 optical flares with $5 \times 10^4s < T_{peak} < 10^6s$ and $5 \times 10^4s < T_{Duration} < 10^6s$. The simulated red points of the first bias are far away from the best fitting line in Figure 5, implying the correlation may be affected by instrumental bias. For the second bias, if smooth, longer-lasting flares could be identified, because peak time and duration time are almost on the same order of magnitude, they marginally follows the $T_{Duration} - T_{peak}$ correlation.

4. THE FREQUENCY DISTRIBUTIONS OF FLARE PARAMETERS

In this section, we use the maximum likelihood estimation method (Bauke 2007) to fit the frequency distributions of optical flare parameters, such as $T_{waiting}$, $T_{Duration}$, T_{peak} , T_{rise} and T_{decay} . We investigate the differential distributions of parameters for the optical flares. The differential distribution is chosen as a power-law form

$$\rho(x) = \beta x^{\alpha_x}, \quad (1)$$

where α_x is the power-law index. The occurrence rate of flares in each bin can be calculated from $\rho(x) = N/\Delta x$, where N and Δx are the number of flares in the bin, and the width of the bin, respectively.

We have studied the frequency distributions of X-ray flares in Yi et al. (2016). We focus on the optical flares observed by *Swift* in this paper. There are 119 GRB op-

tical flares in our sample, and 77 of them have redshifts which consist of a sub-sample. For the total sample, we divide the parameter x , which represents the parameter of flares, into 11 bins. Figure 6 shows the differential distributions of the optical flare in the total sample. The points are the observed data with 1σ errors, which are chosen as the Poisson error. The red curves are the optimal fittings derived with the maximum likelihood estimation method. The optimal fitted parameters α_x for the distributions of the waiting time, duration time, peak time, rise time and decay time are 1.24 ± 0.08 , 1.23 ± 0.07 , 1.28 ± 0.09 , 1.31 ± 0.10 and 1.21 ± 0.07 , respectively. The sub-sample is treated with the similar method after the redshift correction, and the optimal fitting results are shown in Figure 7. The optimal fitted parameters α_x for the distributions of waiting time, duration time, peak time, rise time and decay time are 1.30 ± 0.11 , 1.29 ± 0.09 , 1.29 ± 0.10 , 1.27 ± 0.10 and 1.28 ± 0.11 , respectively. Figures 6 and 7 show that the differential distributions of the flare parameters can be well described by power-law functions. We find that both optical flares and X-ray flares have similar statistical distributions, so we suppose optical flares and X-ray flares have a common physical origin, which implies that both of them may be powered by activities of central engines.

5. DISCUSSION

X-ray flares are the most common phenomena in GRB X-ray afterglows. According to the statistical results of X-ray flares, about more than one-third of *Swift* GRBs with remarkable flares. However, the number of flares in the UV/optical are far less than those of X-ray. Therefore, not all the optical flares correspond to X-ray flares. Swenson et al. (2013) applied the Bayesian Information Criterion to analyze the residuals of the fitted UV/optical light curve, and identified 119 unique flaring periods. In this paper, we study the properties of optical flares, comparing them with X-ray flares. We check all the optical light curves of Swenson et al. (2013) and X-ray afterglows. We find that most of GRBs in this sample have notable flares simultaneously observed in the X-ray band, but there are still about a dozen GRBs with no distinct flare activities in X-ray band.

The temporal behaviors of flares are different from the underlying afterglow emissions, however they are well consistent with those of prompt gamma-ray emissions. Therefore, X-ray and optical flares are supposed to be produced by internal emission powered by central engine. Through a comparative of the afterglow observations, there is evidence suggesting that the optical and X-ray flares originate from similar physical processes (Swenson et al. 2010; Li et al. 2012). Most optical flares usually happen at early time after the prompt emission. However, some flares are even occurring at very late time both in the X-ray and the UV/optical, such as GRB 070318 and GRB 090926A. Flares of these two bursts are not only observed at early time, but matching well at late time greater than 10^5 s in both bands. Therefore, the physical origin of both optical and X-ray flares may be similar, and both of them are related to central engine. However, as discussed above, the presence of flares in one band, but not in another is usually seen. We suppose the primary reason is the lower significance of most flares in the lower energy bands. While the X-ray flares are often

easily identified by visual inspection of the light curves, potential optical flares are more often overlooked or dismissed as noise (Swenson et al. 2010; Li et al. 2012; Swenson & Roming 2013). Whether X-ray and optical flares have the same origin remains an important open question, much more observation data are required to answer this question.

Interestingly, other bumps are also occurring in the optical afterglows. But they are different from optical flares. Generally, the onset of GRB afterglow is seen by a smooth bump in early optical afterglow light curve as the fireball shell is decelerated by the circumburst medium. Liang et al. (2010) extensively searched for the afterglow onset bump feature from early afterglow light curves, and 20 optical onset bumps are identified. These optical afterglows have smooth bumps, with the rising index for most GRBs is 1 – 2, and the decay index is 0.44 – 1.77. These afterglow onset features are well consistent with the external-forward shock (FS) model. Another sharp optical bump is produced by the reverse shock (RS) emission. However, the RS emission is rarely appeared in the optical afterglows. At present, only a small fraction of GRBs shows RS emission in optical afterglows. According to the RS model, the theoretical rising index can be steep as 5 in the thin shell case for a constant interstellar medium (Kobayashi 2000, Yi et al. 2013). One interesting case is GRB 041219A, which shows three significantly power-law rise and fall peaks in the optical-IR band. The first optical peak tracking the gamma-ray light curve during the prompt emission can be understood as emission from internal shocks, while the remaining two peaks are produced by RS and FS component, respectively (Blake et al. 2005; Fan et al. 2005b). Another similar burst is GRB 110205A (Gendre et al. 2012). Therefore, the two optical bumps (FS component and RS component) are attributed to the external shock emission, while the optical flares are related to the internal shocks of the central engine. In our analysis, such bumps are not included.

6. CONCLUSIONS

In this paper, we have compiled 119 optical flares of GRBs taken from *Swift*/*UVOT* catalog of Swenson et al. (2013) until December 2010, including 77 flares with redshifts. We studied the parameters of the optical flares, such as the waiting time, duration time, rise time and decay time. We found the waiting times of optical flares range from between 10 s and 10^6 s after the GRB trigger, and the peak time of an optical flare is in the range of 10^2 s to 10^6 s. We also found some tight correlations between these time scales of optical flares. Generally, these tight correlations suggest that longer rise times associate with longer decay times, and also suggest broader optical flares peak at later times. These properties are consistent with the results of X-ray flares, and indicate the structures of optical flares and X-ray flares are similar. However, these correlations may be affected by the instrumental bias, e.g., flares with short durations but at late time are hard to identify by UVOT. We also studied the frequency distributions of the parameters of optical flares. The best-fitting results for the power-law distributions of the parameters of the optical flares are similar with those of X-ray flares. Our results indicate GRB optical flares and X-ray flares may share the similar physical origin, and both of them are related to central engine activities.

We thank the anonymous referee for useful comments and suggestions. We thank En-Wei Liang, Xue-Feng Wu and Jie-Shuang Wang for useful comments and helps. This work is supported by the National Basic Research Program of China (973 Program, grant No. 2014CB845800), the National Natural Science Foundation of China (grants 11422325, 11373022, and 11573014), the Excellent Youth Foundation of Jiangsu Province (BK20140016), China Postdoctoral science foundation (grant No. 2017M612233), Science and Technology Program of QuFu Normal University (xkj201614).

REFERENCES

- Abdo, A. A., Ackermann, M., Ajello, M., et al. 2011, *ApJ*, 734, L27
 Blake, C. H., Bloom, J. S., Starr, D. L., et al. 2005, *Nature*, 435, 181
 Burrows, D. N., Romano, P., Falcone, A., et al. 2005, *Science*, 309, 1833
 Burrows, D. N., Hill, J. E., Nousek, J. A., et al. 2005, *Space Sci. Rev.*, 120, 165
 Campana, S., Tagliaferri, G., Lazzati, D., et al. 2006, *A&A*, 454, 113
 Chincarini, G., Mao, J., Margutti, R., et al. 2010, *MNRAS*, 406, 2113
 Chincarini, G., Moretti, A., Romano, P., et al. 2007, *ApJ*, 671, 1903
 Dănilă, B., Harko, T., & Mocanu, G. 2015, *MNRAS*, 453, 2982
 Dai, Z. G., Wang, X. Y., Wu, X. F., & Zhang, B. 2006, *Science*, 311, 1127
 Falcone, A. D., Burrows, D. N., Lazzati, D., et al. 2006, *ApJ*, 641, 1010
 Falcone, A. D., Morris, D., Racusin, J., et al. 2007, *ApJ*, 671, 1921
 Fan, Y. Z., & Wei, D. M. 2005, *MNRAS*, 364, L42
 Fan, Y. Z., Zhang, B., & Wei, D. M. 2005, *ApJ*, 628, L25
 Gehrels, N., Chincarini, G., Giommi, P., et al. 2004, *ApJ*, 611, 1005
 Gendre, B., Atteia, J. L., Boër, M., et al. 2012, *ApJ*, 748, 59
 Giannios, D. 2006, *A&A*, 455, L5
 Guidorzi, C., Dichiara, S., Frontera, F., et al. 2015, *ApJ*, 801, 57
 Harko, T., Mocanu, G., & Stroia, N. 2015, *Ap&SS*, 357, 84
 Kelly, B. C. 2007, *ApJ*, 665, 1489
 Kobayashi, S. 2000, *ApJ*, 545, 807
 Kumar, P., & Zhang, B. 2015, *Phys. Rep.*, 561, 1
 Li, L., Liang, E.-W., Tang, Q.-W., et al. 2012, *ApJ*, 758, 27
 Liang, E.-W., Li, L., Gao, H., et al. 2013, *ApJ*, 774, 13
 Liang, E.-W., Yi, S.-X., Zhang, J., et al. 2010, *ApJ*, 725, 2209
 Mészáros, P. 2006, *Reports on Progress in Physics*, 69, 2259
 Mészáros, P., & Rees, M. J. 1997, *ApJ*, 476, 232
 Margutti, R., Chincarini, G., Granot, J., et al. 2011, *MNRAS*, 417, 2144
 Molinari, E., Vergani, S. D., Malesani, D., et al. 2007, *A&A*, 469, L13
 Mu, H.-J., Gu, W.-M., Hou, S.-J., et al. 2016, *ApJ*, 832, 161
 Mu, H.-J., Lin, D.-B., Xi, S.-Q., et al. 2016, *ApJ*, 831, 111
 Nousek, J. A., Kouveliotou, C., Grupe, D., et al. 2006, *ApJ*, 642, 389
 Piran, T. 2004, *Reviews of Modern Physics*, 76, 1143
 Romano, P., Moretti, A., Banat, P. L., et al. 2006, *A&A*, 450, 59
 Roming, P. W. A., Koch, T. S., Oates, S. R., et al. 2009, *ApJ*, 690, 163
 Roming, P. W. A., Kennedy, T. E., Mason, K. O., et al. 2005, *Space Sci. Rev.*, 120, 95
 Sari, R., Piran, T., & Narayan, R. 1998, *ApJ*, 497, L17

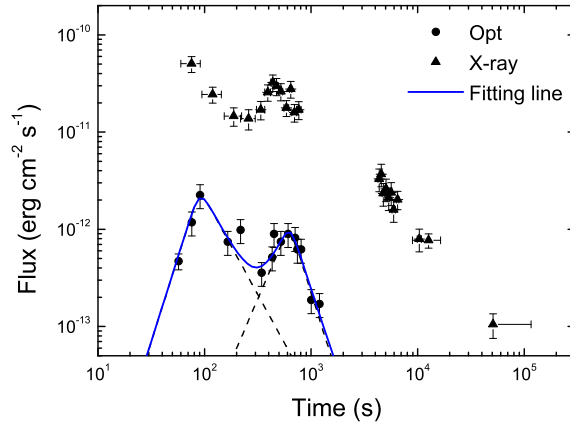


FIG. 1.— The sample of two optical flares of GRB 060926. The two optical cases show the remarkable flare features, which is also corresponding to an X-ray flare, simultaneously.

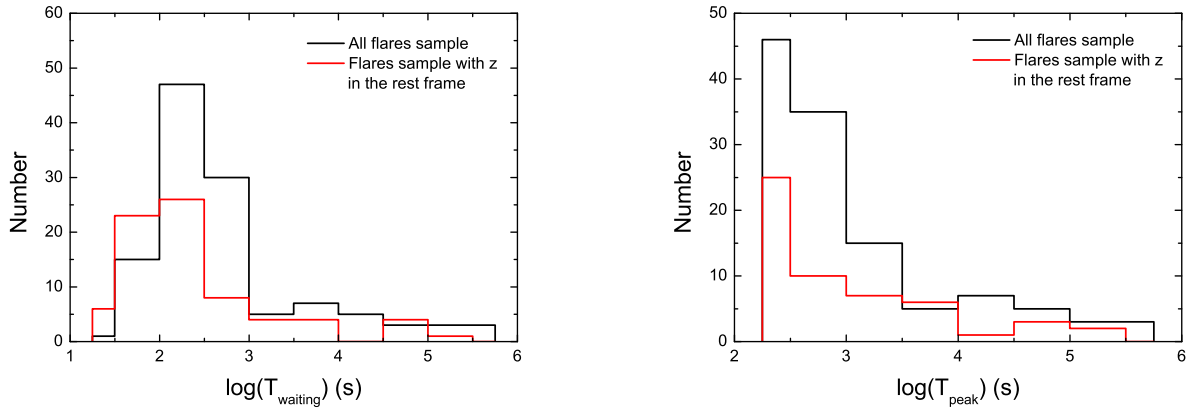


FIG. 2.— The waiting time and peak time distributions of optical flares. The black line is corresponding to all of the sample. The red line represents the flares with redshifts, and the parameters have been transferred to the source frame.

Swenson, C. A., Maxham, A., Roming, P. W. A., et al. 2010, *ApJ*, 718, L14
 Swenson, C. A., & Roming, P. W. A. 2014, *ApJ*, 788, 30
 Swenson, C. A., Roming, P. W. A., De Pasquale, M., & Oates, S. R. 2013, *ApJ*, 774, 2
 Wang, F. Y., & Dai, Z. G. 2013, *Nature Physics*, 9, 465
 Wang, F. Y., Dai, Z. G., Yi, S. X., & Xi, S. Q. 2015, *ApJS*, 216, 8
 Wu, X. F., Dai, Z. G., Wang, X. Y., et al. 2006, 36th COSPAR Scientific Assembly, 36, 731

Yi, S.-X., Wu, X.-F., & Dai, Z.-G. 2013, *ApJ*, 776, 120
 Yi, S.-X., Wu, X.-F., Wang, F.-Y., & Dai, Z.-G. 2015, *ApJ*, 807, 92
 Yi, S.-X., Xi, S.-Q., Yu, H., et al. 2016, *ApJS*, 224, 20
 Zhang, B. 2007, *ChJAA*, 7, 1
 Zhang, B., Fan, Y. Z., Dyks, J., et al. 2006, *ApJ*, 642, 354
 Zhang, B., & Yan, H. 2011, *ApJ*, 726, 90

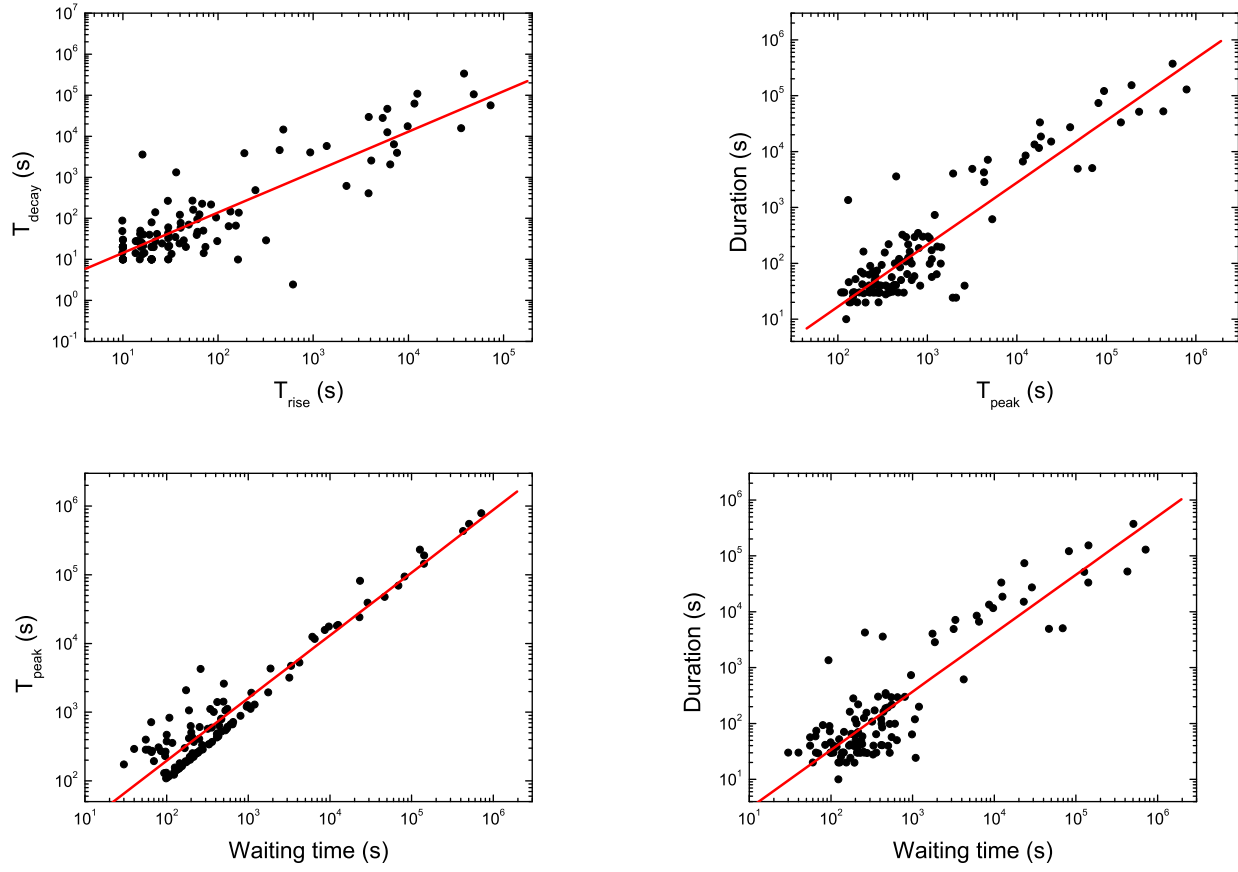


FIG. 3.— The correlations between time scales of GRB optical flares. The rise time is correlated with the decay time, and the duration is correlated with the peak time, which are consistent with the results of X-ray flares. The red line is the best fitting, which is shown in Table 1.

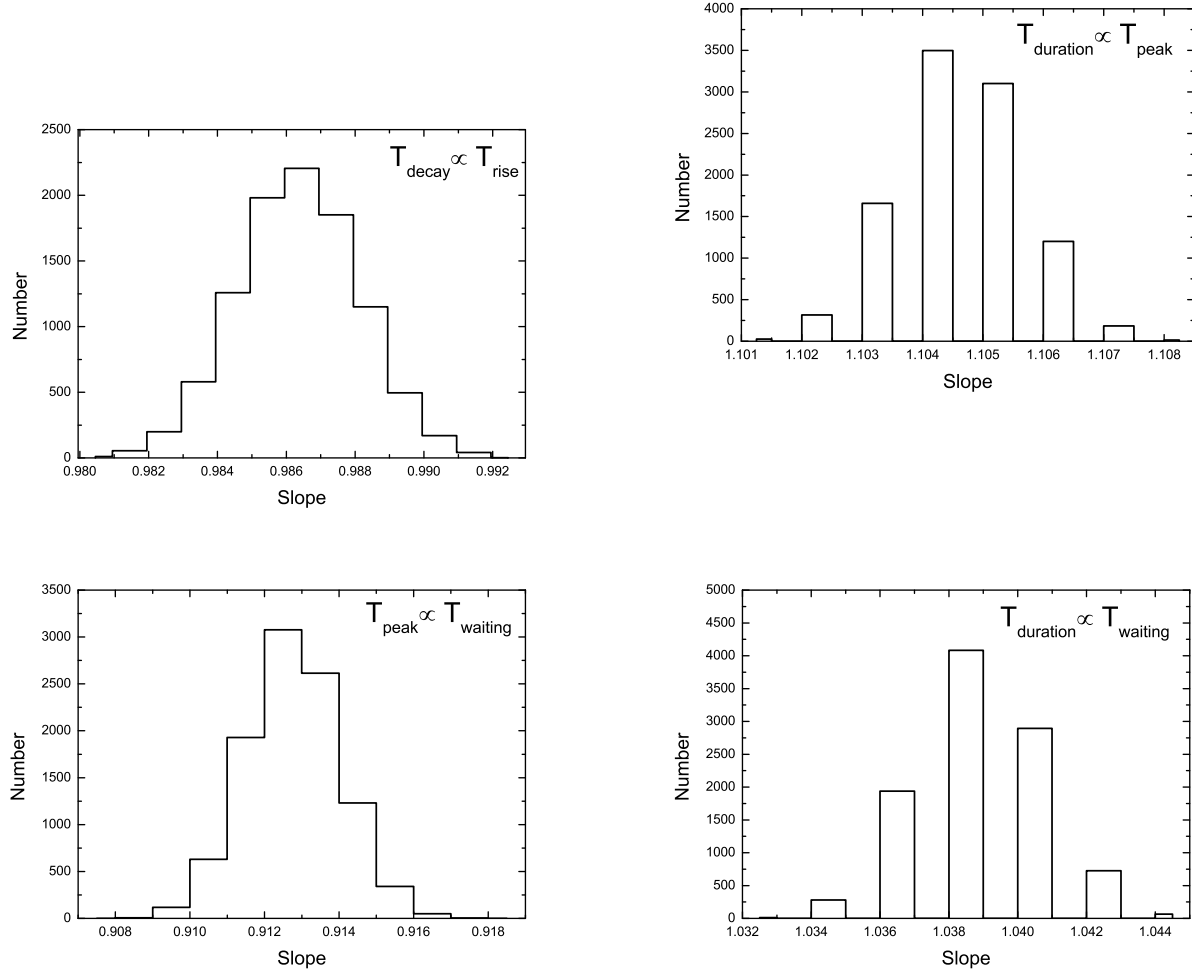


FIG. 4.— The distributions of the best fitting results for the four correlations from simulation data. We simulate 10^4 times for each correlation.

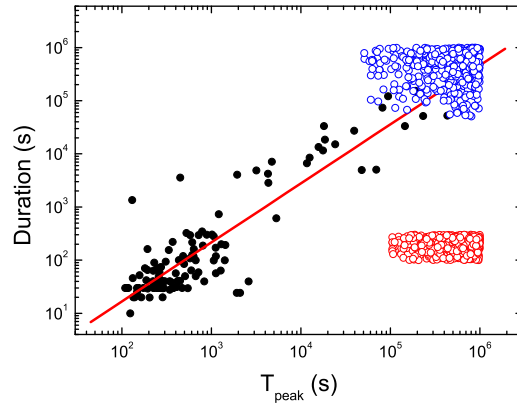


FIG. 5.— Two simulations for the instrumental and observational biases for the $T_{Duration} - T_{peak}$ correlation: flares with short duration times at late times (the red circles) and smooth, longer-lasting flares (the blue circles). It's obviously that the instrumental bias is significant.

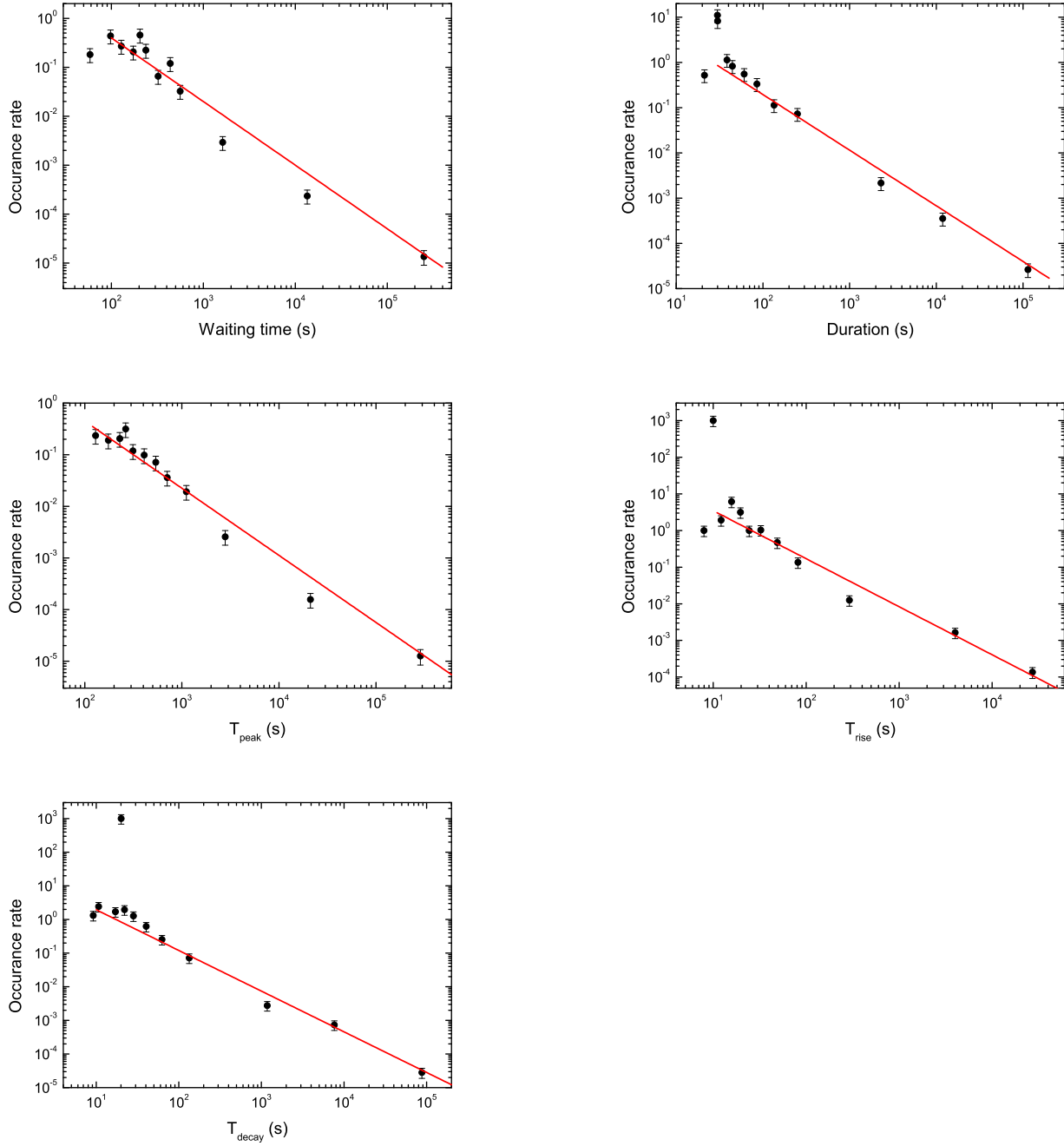


FIG. 6.— The differential distributions of GRB optical flares. 119 GRB optical flares are used. The best-fitting indices for the differential distributions of the waiting time, duration time, peak time, rise time and decay time of the optical flares are 1.24 ± 0.08 , 1.23 ± 0.07 , 1.28 ± 0.09 , 1.31 ± 0.10 and 1.21 ± 0.07 , respectively.

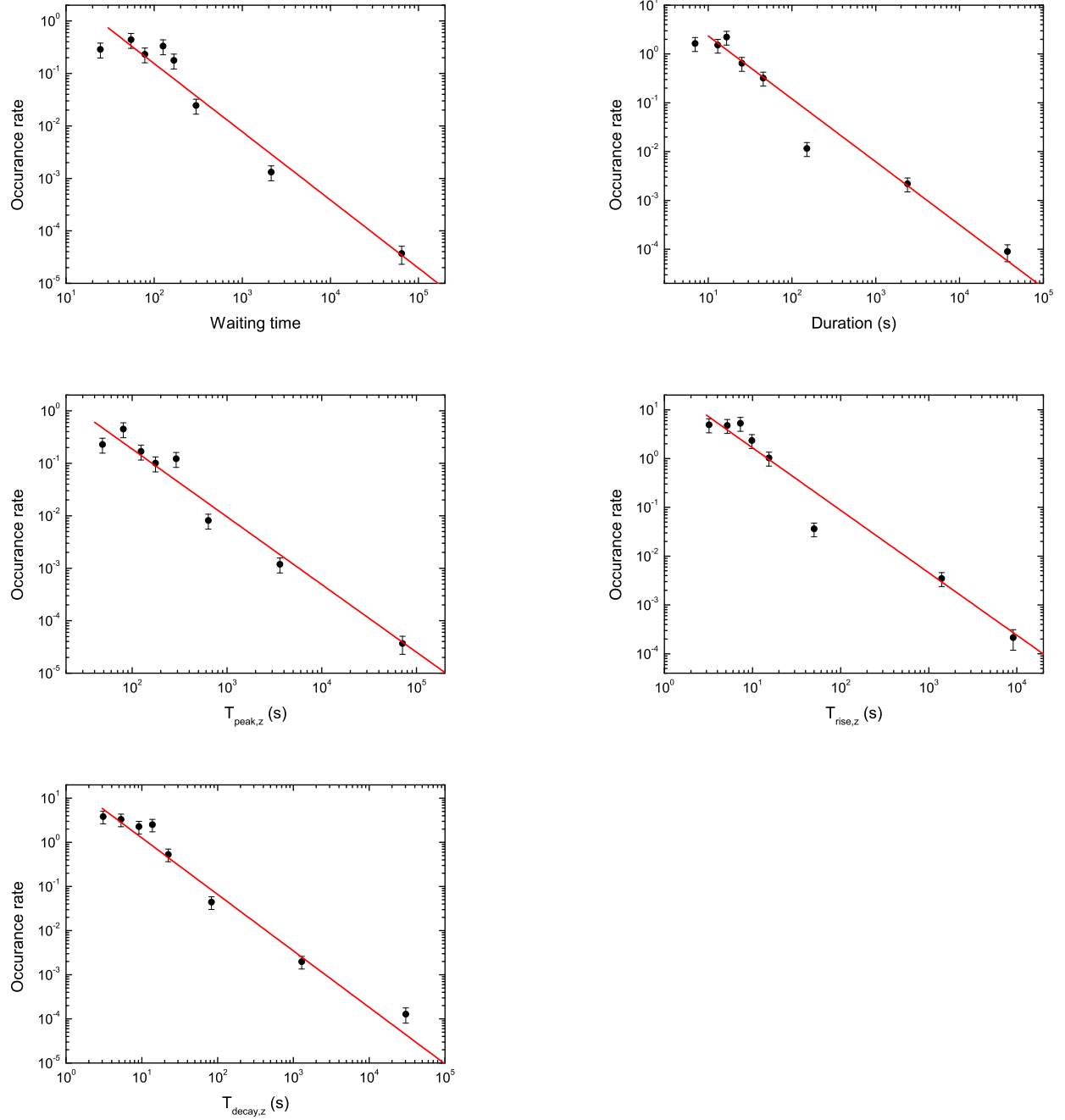


FIG. 7.— The differential distributions of 77 GRB optical flares with redshifts. The best-fitting indices for the differential distributions of the waiting time, duration time, peak time, rise time and decay time of optical flares are 1.30 ± 0.11 , 1.29 ± 0.09 , 1.29 ± 0.10 , 1.27 ± 0.10 and 1.28 ± 0.11 , respectively.

TABLE 1

RESULTS OF THE LINEAR REGRESSION ANALYSIS FOR OPTICAL FLARES. R IS THE SPEARMAN CORRELATION COEFFICIENT, P IS THE CHANCE PROBABILITY, AND δ IS THE CORRELATION DISPERSION.

Correlations	Expressions	R	P	δ
$T_{decay}(T_{rise})$	$\log T_{decay} = (0.17 \pm 0.11) + (0.99 \pm 0.05) \times \log T_{rise}$	0.87	$< 10^{-4}$	0.57
$T_{duration}(T_{peak})$	$\log T_{duration} = (-1.00 \pm 0.15) + (1.11 \pm 0.05) \times \log T_{peak}$	0.91	$< 10^{-4}$	0.45
$T_{peak}(T_{waiting})$	$\log T_{peak} = (0.47 \pm 0.07) + (0.91 \pm 0.03) \times \log T_{waiting}$	0.96	$< 10^{-4}$	0.26
$T_{duration}(T_{waiting})$	$\log T_{duration} = (-0.56 \pm 0.14) + (1.05 \pm 0.05) \times \log T_{waiting}$	0.90	$< 10^{-4}$	0.48